

Research Article

Highly efficient photo-induced surface enhanced Raman spectroscopy from ZnO/Au nanorods



Van Tan Tran^a, Thi Ha Tran^{a,b}, Minh Phuong Le^a, Nguyen Hai Pham^a, Viet Tuyen Nguyen^{a,*},
 Danh Bich Do^c, Xuan Truong Nguyen^d, Bui Nguyen Quoc Trinh^e, Thi Thanh Van Nguyen^f,
 Van Thanh Pham^a, Manh Quynh Luu^a, An Bang Ngac^{a,**}

^a Faculty of Physics, University of Science, Vietnam National University, Hanoi, 334 Nguyen Trai, Thanh Xuan, Hanoi, Viet Nam

^b Faculty of Basic Sciences, Hanoi University of Mining and Geology, 18 Vien Street, Duc Thang Ward, Bac Tu Liem, Hanoi, Viet Nam

^c Faculty of Physics, Hanoi National University of Education, 136 Xuan Thuy, Cau Giay, 100000, Hanoi, Viet Nam

^d School of Chemical Engineering, Hanoi University of Science and Technology, Hanoi, Viet Nam

^e Nanotechnology Program, Faculty of Advanced Technologies and Engineering, Vietnam Japan University, Vietnam National University, Hanoi, Luu Huu Phuoc, Nam Tu Liem, Hanoi, Viet Nam

^f Vietnam Academy of Cryptography Techniques, 141 Chien Thang, Tan Trieu, Thanh Tri, Hanoi, Viet Nam

ARTICLE INFO

Keywords:

ZnO/Au nanorod
 Hydrothermal
 Galvanic
 SERS
 UV excitation

ABSTRACT

Surface-enhanced Raman spectroscopy (SERS) has been widely applied as a useful tool to analyze environmental pollutants, explosives and biomolecules at low concentrations. In recent years, a new approach to further improve sensitivity of SERS measurement is Photo Induced Enhanced Raman scattering (PIERS), where samples are excited by appropriate light before or during Raman measurement. In this study, we successfully fabricated SERS substrates with good sensitivity based on ZnO/Au nanorods by facile galvanic assisted hydrothermal and sputtering techniques. Raman signal can also be further improved conveniently and efficiently by in situ UV-excitation compared with traditional SERS measurement. This approach provides a robust, fast technique for detection of substances at low concentration.

1. Introduction

At present, surface-enhanced Raman spectroscopy (SERS) is a highly sensitive technique, which has been widely applied in fields such as: medical field [1], environmental monitoring [2], food safety [3], etc. The enhancement of Raman signal derives from two main mechanisms: electromagnetic enhancement (EM) and chemical enhancement (CM). EM derives from localized surface plasmon resonance (LSPR) of precious metal nanostructures, and is the main enhancement factor (EF) of about 10^5 - 10^6 [4,5]. Whereas CM, which often accounts for an EF of less than 10^4 , resulted from charge transfer process between metal nanoparticles and analyte molecules [6].

Because size, morphology and density of noble metal nanostructures play an important role in LSPR effect, which in turn determines the enhancement yield, optimization of materials served as SERS substrates has gained much interest from scientists and engineers. Many ideas and strategies have been presented in order to obtain the maximum total EF.

Some examples of these approaches are: fabricating of noble metal nanostructures in various form such as particles [4,7-9], hexagonal arrays [10], pyramid [11], urchin [12], etc., combining noble metal and semiconductor in nanocomposite to take advantages of the unique properties of both materials [5,13], decorating metal nanoparticles on arrays of 1D nanostructures of semiconductor materials to increase hot spot density for SERS [14-16]. However, optimization of materials can only offer a certain EF, and room for advancement of EF by materials design is limited. Therefore, seeking additional methods to enhance the Raman signal related to the measurement process rather than material engineering is necessary because they can help to lower the limit of detection in analytical process based on SERS.

Nanocomposites of ZnO and noble metals are promising materials for fabricating SERS substrates [17-19]. In recent studies, Photo Induced Surface Enhanced Raman spectroscopy has emerged as a novel, facile technique that can enhance SERS intensity efficiently. The studies have shown that before or during Raman measurement, if the sample is

* Corresponding author.

** Corresponding author.

E-mail addresses: nguyenviettuyen@hus.edu.vn (V.T. Nguyen), ngacabang@hus.edu.vn (A.B. Ngac).

excited with an appropriate light, the SERS signal will be clearly intensified [20–24]. Even though some material designs have been developed for PIERS, there are very few studies in the literature that have used ZnO/Au nanorods as photo active SERS substrate. Further more, most studies focus on pre-treatment of SERS substrates with UV radiation. Only few researches mentioned about in situ excitation of the sample during Raman measurement.

In this paper, we report UV-induced surface enhanced Raman scattering from well aligned ZnO/Au nanorods. ZnO/Au nanorods offer a great signal enhancement, which is further amplified up to 30.1 fold under in-situ UV excitation.

2. Experiment

In this experiment, ZnO nanorods were fabricated on print circuit boards (PCB) substrate by galvanic effect assisted hydrothermal method. The oxide layer was first removed by polishing the PCB substrate with fine sand paper then washed with acetone, ethanol and distilled water twice by ultrasonic bath.

A thin layer of aluminum foil is wrapped on the PCB substrate. An empty area of 5×5 mm was left at the center to form galvanic cell structure for the growth of ZnO nanorods. The treated PCB substrates were then dipped into a mixture of 30 ml of 75 mM zinc nitrate $Zn(NO_3)_2$ and 30 ml of 75 mM hexamethylenetetramine (HMTA) $C_6H_{12}N_4$. The reaction temperature was maintained at $90^\circ C$ and the nanorods were grown in 3 h. The Al layer was then removed and the sample was rinsed with distilled water and dried by nitrogen blowing. The synthetic parameters were obtained from our previous studies [16,25] to obtain well aligned ZnO nanorods. ZnO/Au nanorods were then prepared by sputtering gold on the as-synthesized ZnO nanorods by a DC sputtering system (JEOL JFC – 1200). Sputtering time was varied from 20 s to 40 s with sputtering current of 20 mA.

To study the structure of the sample, the XRD measurements were carried out on Panalytical Empyrean diffraction system with a wavelength $K\alpha = 1.54056 \text{ \AA}$. Surface morphology was investigated using Scanning Electron microscope from JEOL (JSM – IT100). SERS and PIERS effects were studied by using Horiba Jobin Yvon's HR 800 Raman spectrometer. A He - Ne laser source with wavelength 632.8 nm was used to excite the samples. Methylene blue (MB) was used as Raman probe. 50 μ l of MB at different concentration was dropped on the samples. After being dried naturally, the samples were ready for Raman measurements. To investigate PIERS effect, the samples were illuminated by an UV LED with a wavelength of 365 nm and power of 1 mW during a measurement. The distance from the LED to the sample surface is 10 cm. The power density at the sample surface was estimated as 0.2 mW/cm^2 . Normal SERS and PIERS spectra were collected at the same spot on the sample to identify the contribution of UV excitation to Raman enhancement.

3. Results and discussion

X-ray diffraction pattern of the prepared ZnO nanorods is shown in Fig. 1. The position of diffraction peaks in the diagram matches well with those of JSPDS card no. 36 - 1451 of ZnO wurzite hexagonal lattice. Apart from the peaks of Cu from the PCB substrate, no other peaks related to impurities was observed in the diagram. Clear diffraction peaks imply the good crystallinity of the sample. The strong intensity of (002) peak resulted from preferential orientation of the obtained nanostructures. The estimated lattice constants of the sample: $a = 0.32$ nm; $c = 0.52$ nm, agree with the values reported in literature for ZnO materials [16,26].

Fig. 2 shows Raman spectrum of ZnO nanorods. The observed peaks at 96 cm^{-1} and 435 cm^{-1} can be assigned to E_2^{low} and E_2^{high} characteristic modes of ZnO. The peak at 96 cm^{-1} is derived from the oscillations of lattice of Zn atoms while the peak at 435 cm^{-1} is related to the vibrations of the oxygen atoms. Other broad peaks associated with defects

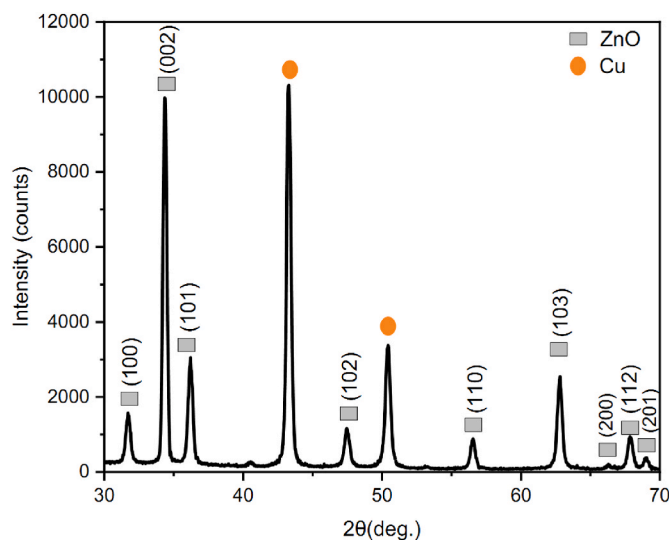


Fig. 1. X-ray diffraction pattern of ZnO rods.

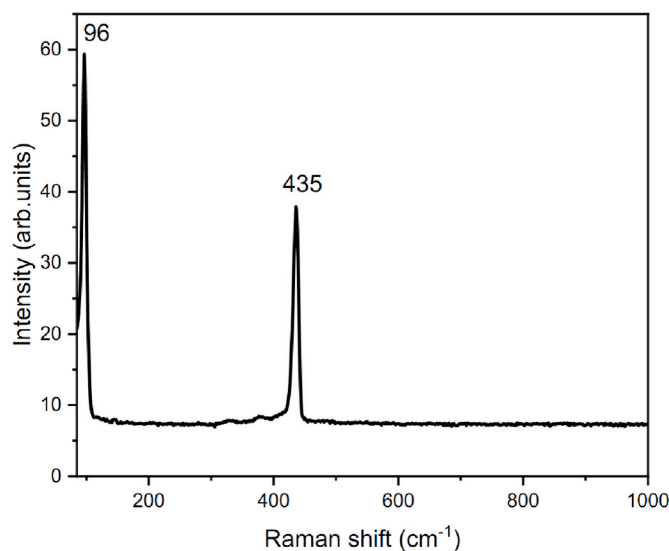


Fig. 2. Raman spectrum of ZnO nanorods.

such as 275 , 539 or 584 cm^{-1} can not be observed in the spectrum. The Raman data demonstrate the high crystallinity of the prepared ZnO nanorods, which is in good agreement with XRD measurement.

Fig. 3a is SEM image of ZnO nanorods (top view). It can be seen that the nanorods are of high density, uniform size and shape with good preferential orientation perpendicular to the substrate. The average diameter of the nanorods is about 300 nm. SEM image of ZnO/Au nanorods (Fig. 3b) clearly show the even distribution of Au nanoparticles on the ZnO nanorods.

EDS measurement result is presented in Fig. 4. The EDS data shows that the obtained ZnO/Au nanorods are free of impurities. Besides signal of copper from PCB substrate, only peaks corresponding to Zn, O, and Au elements can be observed.

Fig. 5 shows the Raman spectra of MB measured on ZnO/Au nanorods prepared with different sputtering time. Among characteristic Raman peaks of MB, the highest peaks were observed at 1388 cm^{-1} , 1616 cm^{-1} . Raman results clearly show that the better enhancement is achieved with sputtering time of 30 s. This result agree well with previous study [16], which showed that sputtering time of higher than 30 s may lead to decreased enhancement. This result can be understood as

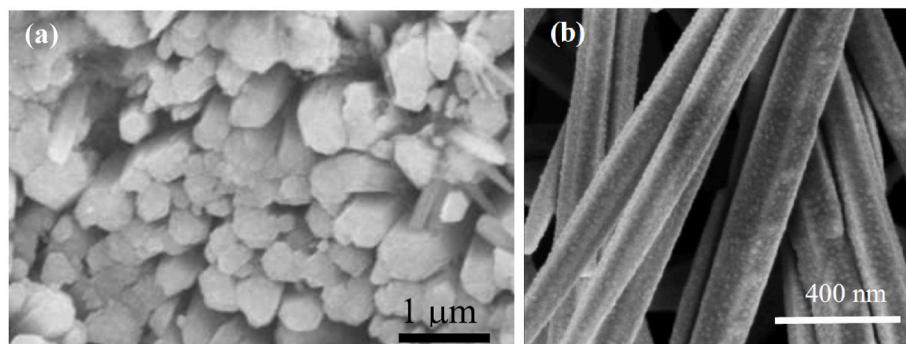


Fig. 3. SEM image of (a) ZnO nanorods and (b) ZnO/Au nanorods prepared with sputtering time of 30 s(b).

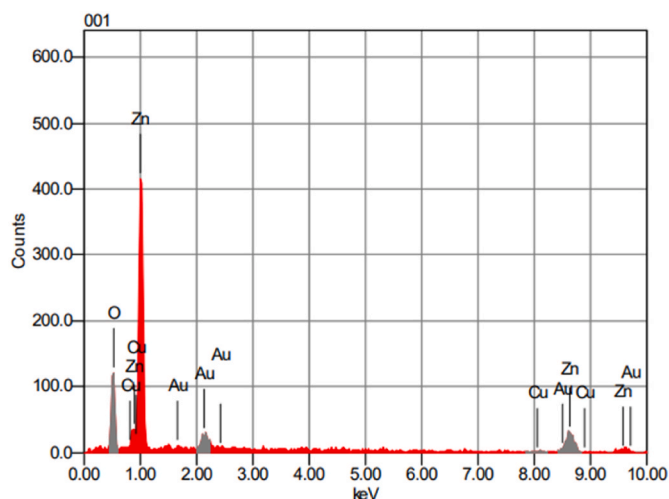


Fig. 4. EDS spectrum of ZnO/Au nanorods.

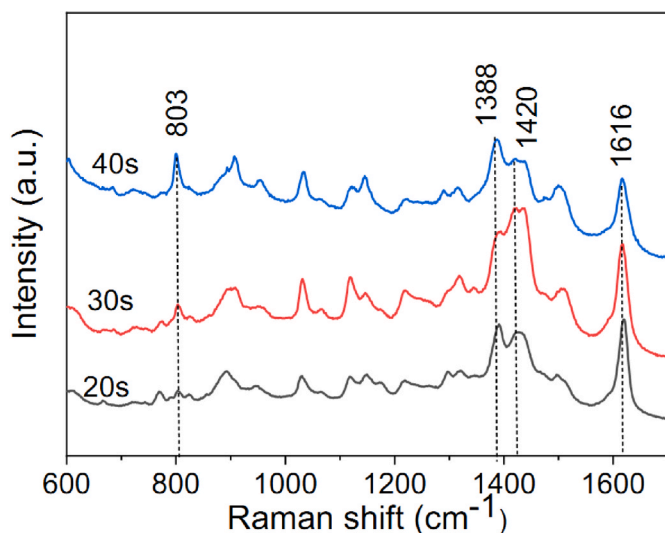


Fig. 5. Surface enhanced Raman spectra of MB measured on ZnO/Au nanorods prepared with different sputtering time.

follow: short sputtering time of 20 s leads to low density of gold nanoparticles on the surface of ZnO nanorods, and results in a lower enhancement coefficient compared to that of sample prepared with sputtering time of 30 s. Sputtering time of 40 s on the other hand produces large island or even continuous shell on the surface of ZnO

nanorods and limits the enhancement capacity of the ZnO/Au nanorods.

After UV excitation, the Raman spectra of MB showed remarkably changes. The Raman intensity was much higher under in situ UV irradiation. Additional featured peaks were observed clearly under photo-induced condition. The ZnO/Au sample with optimal sputtering time of 30 s showed significantly improved PIERS enhancement (Fig. 6). The photo-induced EFs of 30.1; 19.7; 20.9 and 6.0 estimated for peaks at 803, 1509 1119, 1616 cm^{-1} , respectively, are higher than those reported in other studies (Table 1).

The additional enhancement of Raman signal under UV excitation is normally attributed to the generation of oxygen vacancies in semiconductor oxides [21–23]. In order to obtain formation of significant density of defects, the samples are usually pre-irradiated in quite a long time from several tens of minutes to hours before Raman measurement. In our study, PIERS effect was observed under in situ condition, where the sample was shone with UV light in several tens of seconds during Raman measurement. Hence, we believe that generation of electrons and holes in ZnO nanorods under UV irradiation and charge separation due to hetero-junction potential between ZnO and Au are mainly responsible for such efficient amplification of SERS signal in our case. However, defect induced mechanism can not be excluded completely. Additional measurement was performed to confirm this hypothesis. SERS spectra of 10^{-6} M MB were first collected on ZnO/Au nanorods without UV irradiation and with UV irradiation. After that, the spectrum was recollected while UV light was removed. As can be seen in Fig. 7, the relaxation process of Raman signal was observed. After shutting down UV light, Raman signal of MB drops to value before measurement with

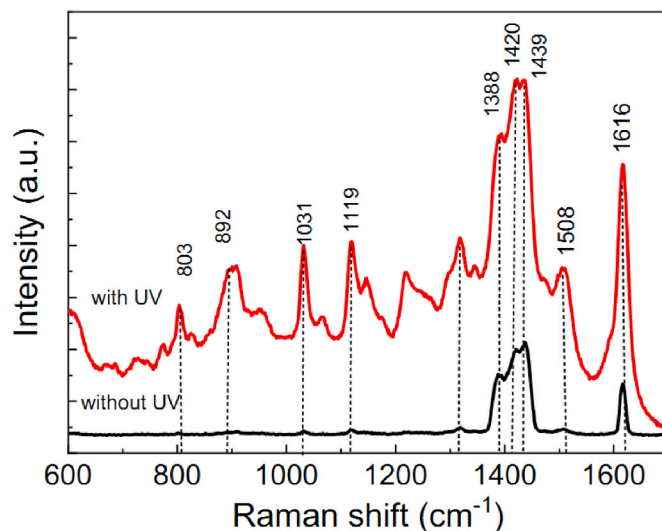


Fig. 6. Raman spectra of MB 10^{-6} M measure on ZnO/Au nanorods with and without UV irradiation.

Table 1
PIERS enhancement factors reported in literature.

SERS Materials	Authors	PIERS EF
WO ₃ /Au thin film	Glass et al. [27]	1.5
TiO ₂ /Ag nanorod	Tiantian Man et al. [23]	1.5
Si/Au	Sawsan et al. [28]	2.5
Au NPs on ZnO thin film	Barbillon et al. [29]	7.5
Au NPs on diphenylalanine peptide nanotubes	Sawsan et al. [28]	4.5
ZnO/Au nanorods	This work	30.1

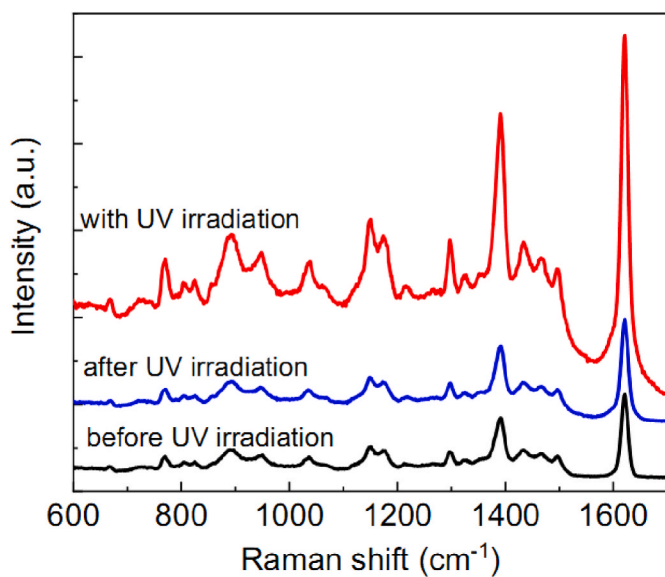


Fig. 7. Relaxation process of Raman signal after UV irradiation.

UV irradiation. This result further supports for enhancement mechanism due to charge transfer in our case.

First, electron-hole pairs are generated in ZnO nanorods under excitation of UV light of energy greater than the bandgap. As the Fermi level of Au is below the Fermi level of ZnO, the Schottky barrier between ZnO and Au facilitates the transfer of electrons from ZnO to Au (Fig. 8). The hot electrons are transferred from the surface plasmon resonance level to MB molecules. At the same time, the accumulation of electron in gold nanostructures can also tune the plasmon resonance properties, which in turn can further enhance the Raman signal. The synergetic enhancement by electromagnetic and chemical mechanism gives rise to such high PIERS EFs as observed.

Enhancement of limit of detection is critical to evaluate SERS substrate performance. Fig. 9 shows Raman spectra of MB of different

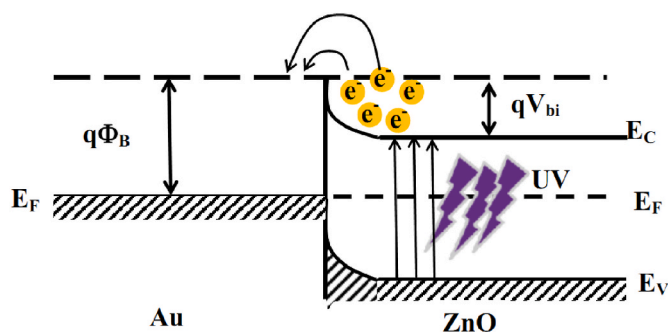


Fig. 8. Charge generation and separation in ZnO/Au nanorods under UV irradiation.

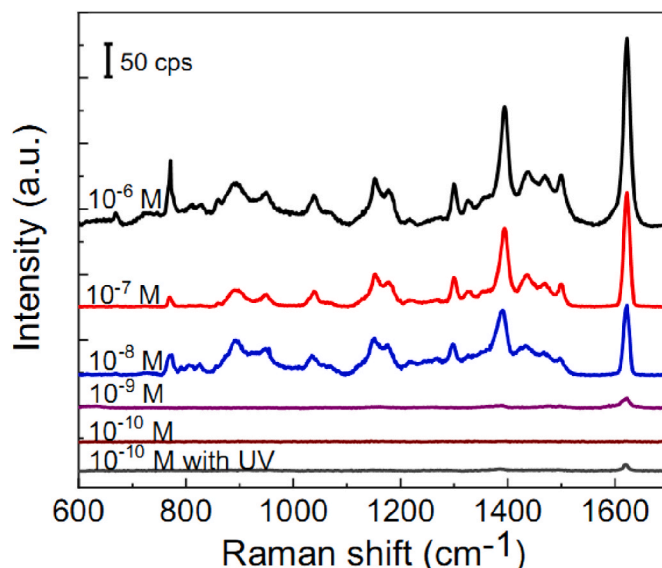


Fig. 9. Raman spectra of MB of different concentrations from: 10^{-6} M down to 10^{-10} M measured on ZnO/Au nanorods without UV irradiation and Raman spectrum of 10^{-10} M MB with UV irradiation.

concentrations from: 10^{-6} M down to 10^{-10} M measured on ZnO/Au nanorods without UV irradiation and Raman spectrum of 10^{-10} M MB with UV irradiation. It can be seen that as the concentration of analyte decreases, the Raman intensity decreases accordingly. The results showed that the lowest concentration of MB that is still detectable on ZnO/Au nanorods is 10^{-9} M. The Raman signal of 10^{-10} M MB can not be resolved from background noise. However, under UV irradiation, characteristic peaks of MB at concentration of 10^{-10} M can be observed clearly. The results show that UV excitation helps to reduce the limit of detection of MB on ZnO/Au SERS substrate.

4. Conclusion

ZnO nanorods of high density, good orientation, uniform size and shape were successfully fabricated by hydrothermal method assisted with galvanic effect. The prepared ZnO/Au nanorods are SERS substrates to enhance Raman scattering with good enhancement and high sensitivity. Upon UV irradiation, the ZnO/Au nanorods exhibit high photo-induced Raman enhancement with 30.1-fold higher intensity compared with normal SERS measurement under the same condition. The combination of plasmonic nanoparticles with photo-activated semiconductor based substrates offers improved sensitivity beyond the normal SERS effect under photo excitation. The obtained results suggest a simple, effective, potential method to improve the sensitivity and reduce the detection limit of substances on the basis of enhanced Raman measurement. The advantages of ZnO/Au nanorods based SERS substrates including low cost; simple preparation, high sensitivity are promising in many fields such as environment monitoring, food safety, medical field, etc.

CRediT authorship contribution statement

Van Tan Tran: Data curation, Investigation, Visualization, Writing - original draft. **Thi Ha Tran:** Conceptualization, Investigation, Methodology, Data curation, Supervision, Writing - original draft. **Minh Phuong Le:** Investigation. **Nguyen Hai Pham:** Conceptualization, Supervision, Writing - review & editing. **Viet Tuyen Nguyen:** Conceptualization, Investigation, Data curation, Methodology, Supervision, Writing - review & editing. **Danh Bich Do:** Investigation. **Xuan Truong Nguyen:** Investigation. **Bui Nguyen Quoc Trinh:** Investigation. **Thi Thanh Van Nguyen:** Investigation. **Van Thanh Pham:** Investigation,

Project administration, Resources, Funding acquisition. **Manh Quynh Luu**: Investigation, Resources. **An Bang Ngac**: Conceptualization, Methodology, Data curation, Writing – review & editing.

Declaration of competing interest

The authors declare that they have no known competing financial interests or personal relationships that could have appeared to influence the work reported in this paper.

Data availability

Data will be made available on request.

Acknowledgement

This research is funded by Vietnam National Foundation for Science and Technology Development (NAFOSTED) under grant number 103.99–2020.33. Ms. Thi Ha Tran would like to thank the PhD Scholarship Fund of Vietnam National University, code VNU.2021.03.

References

- [1] V. Moisoiu, S.D. Iancu, A. Stefanu, T. Moisoiu, B. Pardini, M.P. Dragomir, N. Crisan, L. Avram, D. Crisan, I. Andras, D. Fodor, L.F. Leopold, C. Socaciu, Z. Bálint, C. Tomuleasa, F. Elec, N. Leopold, SERS liquid biopsy: an emerging tool for medical diagnosis, *Colloids Surf. B Biointerfaces* 208 (2021), <https://doi.org/10.1016/j.colsurfb.2021.112064>.
- [2] T.T.X. Ong, E.W. Blanch, O.A.H. Jones, Surface Enhanced Raman Spectroscopy in environmental analysis, monitoring and assessment, *Sci. Total Environ.* 720 (2020), 137601, <https://doi.org/10.1016/j.scitotenv.2020.137601>.
- [3] L. Jiang, M.M. Hassan, S. Ali, H. Li, R. Sheng, Q. Chen, Evolving trends in SERS-based techniques for food quality and safety: a review, *Trends Food Sci. Technol.* 112 (2021) 225–240, <https://doi.org/10.1016/j.tifs.2021.04.006>.
- [4] T.H.T. Nguyen, T.M.A. Nguyen, C.D. Sai, T.H.Y. Le, T.N. Anh Tran, T.C. Bach, V. V. Le, N.H. Pham, A.B. Ngac, V.T. Nguyen, T.H. Tran, Efficient surface enhanced Raman scattering substrates based on complex gold nanostructures formed by annealing sputtered gold thin films, *Opt. Mater.* 121 (2021), 111488, <https://doi.org/10.1016/j.optmat.2021.111488>.
- [5] T.H. Tran, T.M.A. Nguyen, V.P.T. Dao, C.D. Sai, T.C. Bach, N.H. Pham, A.B. Ngac, V.T. Pham, T.K.C. Tran, H. Cheong, V.T. Nguyen, Highly sensitive characteristic of surface enhanced Raman scattering for CuO/Au core/shell nanowires substrate, *Ceram. Int.* 48 (2022) 3199–3205, <https://doi.org/10.1016/j.ceramint.2021.10.093>.
- [6] S. Schlücker, Surface-enhanced Raman spectroscopy: concepts and chemical applications, *Angew. Chemie - Int. Ed.* 53 (2014) 4756–4795, <https://doi.org/10.1002/anie.201205748>.
- [7] H. Liu, A.M. Schwenke, F. Kretschmer, S. Hoepfner, U.S. Schubert, Gold nanoparticle cluster Arrays for high-performance SERS substrates fabricated by electro-oxidative lithography, *ChemNanoMat* 2 (2016) 781–785, <https://doi.org/10.1002/cnma.201600063>.
- [8] J.S. Hwang, M. Yang, Sensitive and reproducible gold SERS sensor based on interference lithography and electrochemical deposition, *Sensors* (2018) 18, <https://doi.org/10.3390/s18114076>.
- [9] A. Vincenzo, P. Roberto, F. Marco, M.M. Onofrio, I. Maria Antonia, Surface plasmon resonance in gold nanoparticles: a review, *J. Phys. Condens. Matter* 29 (2017), 203002. <http://stacks.iop.org/0953-8984/29/i=20/a=203002>.
- [10] E. Gürdal, S. Dickreuter, F. Noureddine, P. Bieschke, D.P. Kern, M. Fleischer, Self-assembled quasi-hexagonal arrays of gold nanoparticles with small gaps for surface-enhanced Raman spectroscopy, *Beilstein J. Nanotechnol.* 9 (2018) 1977–1985, <https://doi.org/10.3762/bjnano.9.188>.
- [11] C. Zhang, S.Z. Jiang, Y.Y. Huo, A.H. Liu, S.C. Xu, X.Y. Liu, Z.C. Sun, Y.Y. Xu, Z. Li, B.Y. Man, SERS detection of R6G based on a novel graphene oxide/silver nanoparticles/silicon pyramid arrays structure, *Opt Express* 23 (2015), 24811, <https://doi.org/10.1364/oe.23.024811>.
- [12] Q. Huang, J. Li, Enhanced photocatalytic and SERS properties of ZnO/Ag hierarchical multipods-shaped nanocomposites, *Mater. Lett.* 204 (2017) 85–88, <https://doi.org/10.1016/j.matlet.2017.06.019>.
- [13] T.H. Tran, M.H. Nguyen, T.H.T. Nguyen, V.P.T. Dao, Q.H. Nguyen, C.D. Sai, N. H. Pham, T.C. Bach, A.B. Ngac, T.T. Nguyen, K.H. Ho, H. Cheong, V.T. Nguyen, Facile fabrication of sensitive surface enhanced Raman scattering substrate based on CuO/Ag core/shell nanowires, *Appl. Surf. Sci.* 509 (2020), 145325, <https://doi.org/10.1016/j.apsusc.2020.145325>.
- [14] C. Zhang, C. Li, J. Yu, S. Jiang, S. Xu, C. Yang, Y.J. Liu, X. Gao, A. Liu, B. Man, SERS activated platform with three-dimensional hot spots and tunable nanometer gap, *Sensor. Actuator. B Chem.* 258 (2018) 163–171, <https://doi.org/10.1016/j.snb.2017.11.080>.
- [15] J. Xu, C. Li, H. Si, X. Zhao, L. Wang, S. Jiang, D. Wei, J. Yu, X. Xiu, C. Zhang, 3D SERS substrate based on Au-Ag bi-metal nanoparticles/MoS₂ hybrid with pyramid structure, *Opt Express* 26 (2018), 21546, <https://doi.org/10.1364/oe.26.021546>.
- [16] Q.K. Doan, M.H. Nguyen, C.D. Sai, V.T. Pham, H.H. Mai, N.H. Pham, T.C. Bach, V. T. Nguyen, T.T. Nguyen, K.H. Ho, T.H. Tran, Enhanced optical properties of ZnO nanorods decorated with gold nanoparticles for self cleaning surface enhanced Raman applications, *Appl. Surf. Sci.* 505 (2020), 144593, <https://doi.org/10.1016/j.apsusc.2019.144593>.
- [17] J. Lu, C. Xu, H. Nan, Q. Zhu, F. Qin, A.G. Manohari, M. Wei, Z. Zhu, Z. Shi, Z. Ni, SERS-active ZnO/Ag hybrid WGM microcavity for ultrasensitive dopamine detection, *Appl. Phys. Lett.* 109 (2016), <https://doi.org/10.1063/1.4961116>.
- [18] C. Huang, C. Xu, J. Lu, Z. Li, Z. Tian, 3D Ag/ZnO hybrids for sensitive surface-enhanced Raman scattering detection, *Appl. Surf. Sci.* 365 (2016) 291–295, <https://doi.org/10.1016/j.apsusc.2016.01.026>.
- [19] Z. Huang, Y. Yan, C. Xing, Q. Wang, J. Li, Y. Zhang, Y. Zeng, Y. Zhao, Y. Jiang, Enhanced properties of hierarchically-nanostructured undoped acceptor-rich ZnO single-crystal microtube irradiated by UV laser, *J. Alloys Compd.* 789 (2019) 841–851, <https://doi.org/10.1016/j.jallcom.2019.03.117>.
- [20] M. Zhang, H. Sun, X. Chen, J. Yang, L. Shi, T. Chen, Y. Bao, J. Liu, Y. Wu, Highly efficient photoinduced enhanced Raman spectroscopy (PIERS) from plasmonic nanoparticles decorated 3D semiconductor arrays for ultrasensitive, portable, and recyclable detection of organic pollutants, *ACS Sens.* 4 (2019) 1670–1681, <https://doi.org/10.1021/acssensors.9b00562>.
- [21] A. Brognara, B.R. Bricchi, L. William, O. Brinza, M. Konstantakopoulou, A.L. Bassi, M. Ghidelli, N. Lidgi-Guigui, New mechanism for long photo-induced enhanced Raman spectroscopy in Au nanoparticles embedded in TiO₂, *Small* 18 (2022), 2201088, <https://doi.org/10.1002/sml.202201088>.
- [22] J. Zhao, Z. Wang, J. Lan, I. Khan, X. Ye, J. Wan, Y. Fei, S. Huang, S. Li, J. Kang, Recent advances and perspectives in photo-induced enhanced Raman spectroscopy, *Nanoscale* 13 (2021) 8707–8721, <https://doi.org/10.1039/d1nr01255j>.
- [23] T. Man, W. Lai, M. Xiao, X. Wang, A.R. Chandrasekaran, H. Pei, L. Li, A versatile biomolecular detection platform based on photo-induced enhanced Raman spectroscopy, *Biosens. Bioelectron.* 147 (2020), <https://doi.org/10.1016/j.bios.2019.111742>.
- [24] S. Ben-Jaber, W.J. Peveler, R. Quesada-Cabrera, E. Cortés, C. Sotelo-Vazquez, N. Abdul-Karim, S.A. Maier, I.P. Parkin, Photo-induced enhanced Raman spectroscopy for universal ultra-trace detection of explosives, pollutants and biomolecules, *Nat. Commun.* 7 (2016) 1–6, <https://doi.org/10.1038/ncomms12189>.
- [25] H.H. Mai, V.T. Pham, V.T. Nguyen, C.D. Sai, C.H. Hoang, T.B. Nguyen, Non-enzymatic fluorescent biosensor for glucose sensing based on ZnO nanorods, *J. Electron. Mater.* 46 (2017) 3714–3719, <https://doi.org/10.1007/s11664-017-5300-8>.
- [26] T.D. Canh, N.V. Tuyen, N.N. Long, Influence of solvents on the growth of zinc oxide nanoparticles fabricated by microwave irradiation, *VNU J. Sci. Math. - Phys.* 25 (2009) 71–76.
- [27] D. Glass, E. Cortés, S. Ben-Jaber, T. Brick, W.J. Peveler, C.S. Blackman, C.R. Howle, R. Quesada-Cabrera, I.P. Parkin, S.A. Maier, Dynamics of photo-induced surface oxygen vacancies in metal-oxide semiconductors studied under ambient conditions, *Adv. Sci.* 6 (2019), <https://doi.org/10.1002/advs.201901841>.
- [28] S. Almomammed, F. Zhang, B.J. Rodriguez, J.H. Rice, Photo-induced surface-enhanced Raman spectroscopy from a diphenylalanine peptide nanotube-metal nanoparticle template, *Sci. Rep.* 8 (2018) 41–44, <https://doi.org/10.1038/s41598-018-22269-x>.
- [29] G. Barbillon, T. Noblet, C. Humbert, Highly crystalline ZnO film decorated with gold nanospheres for PIERS chemical sensing, *Phys. Chem. Chem. Phys.* 22 (2020) 21000–21004, <https://doi.org/10.1039/d0cp03902k>.